
Recent Advances in
Microbiology
Dana M. Santos, Ph.D
Editor

Recent Advances in

MICROBIOLOGY

This page intentionally left blank

Recent Advances in

MICROBIOLOGY

Edited By

Dana M. Santos, PhD

Professor, Department of Anthropology,
Binghamton University, State University of New York, U.S.A.

Apple Academic Press

TORONTO NEW YORK

CRC Press
Taylor & Francis Group
6000 Broken Sound Parkway NW, Suite 300
Boca Raton, FL 33487-2742

Apple Academic Press, Inc
3333 Mistwell Crescent
Oakville, ON L6L 0A2
Canada

© 2012 by Apple Academic Press, Inc.
Exclusive worldwide distribution by CRC Press an imprint of Taylor & Francis Group, an Informa business

No claim to original U.S. Government works
Version Date: 20120530

International Standard Book Number-13: 978-1-4665-5845-8 (eBook - PDF)

This book contains information obtained from authentic and highly regarded sources. Reasonable efforts have been made to publish reliable data and information, but the author and publisher cannot assume responsibility for the validity of all materials or the consequences of their use. The authors and publishers have attempted to trace the copyright holders of all material reproduced in this publication and apologize to copyright holders if permission to publish in this form has not been obtained. If any copyright material has not been acknowledged please write and let us know so we may rectify in any future reprint.

Except as permitted under U.S. Copyright Law, no part of this book may be reprinted, reproduced, transmitted, or utilized in any form by any electronic, mechanical, or other means, now known or hereafter invented, including photocopying, microfilming, and recording, or in any information storage or retrieval system, without written permission from the publishers.

For permission to photocopy or use material electronically from this work, please access www.copyright.com (http://www.copyright.com/) or contact the Copyright Clearance Center, Inc. (CCC), 222 Rosewood Drive, Danvers, MA 01923, 978-750-8400. CCC is a not-for-profit organization that provides licenses and registration for a variety of users. For organizations that have been granted a photocopy license by the CCC, a separate system of payment has been arranged.

Trademark Notice: Product or corporate names may be trademarks or registered trademarks, and are used only for identification and explanation without intent to infringe.

Visit the Taylor & Francis Web site at
http://www.taylorandfrancis.com

and the CRC Press Web site at
http://www.crcpress.com

For information about Apple Academic Press product
http://www.appleacademicpress.com

Preface

Microbiology is a broad term for research including any type of microorganism such as bacteria, viruses, fungi, parasites and even prions. Current areas of particular interest to researchers include:

- antibiotics and antivirals
- antibiotic resistance
- bioremediation
- biotechnology

A degree in microbiology is ideal for work in various fields such as disease research, biotechnology, pharmaceuticals, or microbial genetics and systematics.

Understanding the genetics and behavior of disease-causing pathogens plays a crucial role in discovering effective pharmaceuticals, particularly in the face of increasing global antibiotic resistance. Microbiology is also important in present environmental concerns such as the use of microorganisms in bioremediation or energy production.

New diagnostics, pharmaceuticals, and understanding of the basis of disease will continue to be at the forefront of microbiology research. This is particularly relevant in the face of increasing antibiotic resistance. As concern for the state of our environment grows, there is increasing interest in using microorganisms to clean pollution or generate energy.

— Dana M. Santos, PhD

This page intentionally left blank

List of Contributors

N. A. Affara
Department of Pathology, University of Cambridge, Cambridge CB2,1QP, UK.

Misagh Alipour
The Novel Drug and Vaccine Delivery Systems Facility, Department of Chemistry and Biochemistry, Laurentian University, Sudbury, Ontario, Canada.

Ali O. Azghani
Department of Biology, University of Texas at Tyler, Tyler, TX, USA.

Valerio Berardi
Dipartimento di Genetica e Biologia Molecolare, Sapienza Università di Roma, Roma, Italy.

Agata Bielecka
Synthetic and Systems Biology Group, Helmholtz Center for Infection Research (HZI), Braunschweig, Germany.

Marcos Bilen
Laboratorio Ingeniería Genética, Biología Celular y Molecular- LIGBCM, Universidad Nacional de Quilmes, Roque Saenz Peña 352, Bernal, Buenos Aires, Argentina.

Ju Cao
Key Laboratory of Laboratory Medical Diagnostics, Ministry of Education, Faculty of Laboratory Medicine, Chongqing Medical University, Chongqing 400016, P.R. China.

Mauro Castelli
Regina Elena Cancer Institute, Roma, Italy.

O. E. Chausiaux
Department of Pathology, University of Cambridge, Cambridge CB2,1QP, UK.

Younghak Cho
School of Mechanical Design and Automation Engineering, Seoul National University of Technology, Seoul, Korea.

Ricardo S. Corral
Servicio de Parasitología y Enfermedad de Chagas. Hospital de Niños Dr. Ricardo Gutiérrez. Gallo 1330, Ciudad Autónoma de Buenos Aires, Argentina.

Romina A. Cutrullis
Servicio de Parasitología y Enfermedad de Chagas. Hospital de Niños Dr. Ricardo Gutiérrez. Gallo 1330, Ciudad Autónoma de Buenos Aires, Argentina.

Tamás Czárán
Ecology and Theoretical Biology Research Group of the Hungarian Academy of Science and Eötvös University, Budapest, Hungary.

Genevieve Di Bartolo
Genomics Division, DOE Joint Genome Institute, Walnut Creek, CA 94598, USA.
Boards 'N More, Brentwood, CA 94513, USA.

Paul de Figueiredo
Department of Plant Pathology and Microbiology, Texas A&M University, College Station, TX, USA.
Department of Veterinary Pathobiology, Texas A&M University, College Station, TX, USA.

Helene Feil
Department of Plant and Microbial Biology, University of California, Berkeley, CA 94720, USA.
Land for Urban Wildlife, Concord, CA 94527, USA.

William S. Feil
Department of Plant and Microbial Biology, University of California, Berkeley, CA 94720, USA.
Land for Urban Wildlife, Concord, CA 94527, USA.

R. A. Furlong
Department of Pathology, University of Cambridge, Cambridge CB2,1QP, UK.

Gaspare Galati
Dipartimento di Chirurgia "Pietro Valdoni", Roma, Italy.

Miguel Godinho
Synthetic and Systems Biology Group, Helmholtz Center for Infection Research (HZI), Braunschweig, Germany.

Raul O. Gonzalez
Programa de Nanomedicinas, Universidad Nacional de Quilmes, Roque Saenz Peña 352, Bernal, Buenos Aires, Argentina.

Murray Hackett
Department of Chemical Engineering, University of Washington, Seattle, WA, USA.

Majed Halwani
The Novel Drug and Vaccine Delivery Systems Facility, Department of Chemistry and Biochemistry, Laurentian University, Sudbury, Ontario, Canada.

Arum Han
Department of Electrical and Computer Engineering, Texas A&M University, College Station, TX, USA.

Sharifah Syed Hassan
School of Medicine and Health Sciences, Monash University, Sunway Campus, Kuala Lumpur, Malaysia.

Erik L. Hendrickson
Department of Chemical Engineering, University of Washington, Seattle, WA, USA.

Leticia H. Higa
Programa de Nanomedicinas, Universidad Nacional de Quilmes, Roque Saenz Peña 352, Bernal, Buenos Aires, Argentina.

Piotr Hildebrandt
Department of Microbiology, Chemical Faculty, Gdańsk University of Technology, Narutowicza 11/12, 80-952 Gdańsk, Poland.

Rolf F. Hoekstra
Laboratory of Genetics, Wageningen University, Wageningen, The Netherlands.

Huijie Hou
Department of Electrical and Computer Engineering, Texas A&M University, College Station, TX, USA.

Aini Ideris
Institute of Bioscience, University Putra Malaysia, UPM Serdang, Selangor, 43400, Malaysia.
Faculty of Veterinary Medicine, Universiti Putra Malaysia, UPM Serdang, Selangor, 43400, Malaysia.

Alfred Orina Isaac
The Department of Pathology, Case Western Reserve University, Cleveland, OH, USA.

O. Jafer
Department of Pathology, University of Cambridge, Cambridge CB2,1QP, UK.

Fatemeh Jahanshiri
Department of Microbiology, Faculty of Biotechnology and Biomolecular Sciences, University Putra Malaysia, UPM Serdang, Selangor, 43400, Malaysia.

Keith Keller
Physical Biosciences Division, Lawrence Berkeley National Laboratories, Berkeley, CA 94710, USA.

Masae Kuboniwa
Department of Preventive Dentistry, Osaka University Graduate School of Dentistry, Osaka, Japan.

Józef Kur
Department of Microbiology, Chemical Faculty, Gdańsk University of Technology, Narutowicza 11/12, 80-952 Gdańsk, Poland.

Richard J. Lamont
Department of Oral Biology, University of Florida, Gainesville, FL, USA.

Alla Lapidus
Genomics Division, DOE Joint Genome Institute, Walnut Creek, CA 94598, USA.

Lei Li
Department of Plant Pathology and Microbiology, Texas A&M University, College Station, TX, USA.

Nan Li
Key Laboratory of Laboratory Medical Diagnostics, Ministry of Education, Faculty of Laboratory Medicine, Chongqing Medical University, Chongqing 400016, P.R. China.

Youqiang Li
Key Laboratory of Laboratory Medical Diagnostics, Ministry of Education, Faculty of Laboratory Medicine, Chongqing Medical University, Chongqing 400016, P.R. China.

Xiu Luo
The Department of Pathology, Case Western Reserve University, Cleveland, OH, USA.

Vítor A. P. Martins dos Santos
Synthetic and Systems Biology Group, Helmholtz Center for Infection Research (HZI), Braunschweig, Germany.

Maradumane L. Mohan
The Department of Pathology, Case Western Reserve University, Cleveland, OH, USA.

Irma Morelli
Centro de Investigación y Desarrollo en Fermentaciones Industriales-CINDEFI, Facultad de Ciencia Exactas, Universidad Nacional de La Plata, 50 y 115 La Plata, Buenos Aires, Argentina.

Maria Jose Morilla
Programa de Nanomedicinas, Universidad Nacional de Quilmes, Roque Saenz Peña 352, Bernal, Buenos Aires, Argentina.

Siqiang Niu
Key Laboratory of Laboratory Medical Diagnostics, Ministry of Education, Faculty of Laboratory Medicine, Chongqing Medical University, Chongqing 400016, P.R. China.

Matthew A. Oberhardt
Department of Biomedical Engineering, University of Virginia, Health System, Charlottesville, VA, USA.

Abdul Rahman Omar
Institute of Bioscience, University Putra Malaysia, UPM Serdang, Selangor, 43400, Malaysia.
Faculty of Veterinary Medicine, Universiti Putra Malaysia, UPM Serdang, Selangor, 43400, Malaysia.

Abdelwahab Omri
The Novel Drug and Vaccine Delivery Systems Facility, Department of Chemistry and Biochemistry, Laurentian University, Sudbury, Ontario, Canada.

Jason A. Papin
Department of Biomedical Engineering, University of Virginia, Health System, Charlottesville, VA, USA.

Jiri Petrak
Department of Pathological Physiology, First Faculty of Medicine, Charles University in Prague, Prague, Czech Republic.

Patricia B. Petray
Servicio de Parasitología y Enfermedad de Chagas. Hospital de Niños Dr. Ricardo Gutiérrez. Gallo 1330, Ciudad Autónoma de Buenos Aires, Argentina.

Jacek Puchałka
Synthetic and Systems Biology Group, Helmholtz Center for Infection Research (HZI), Braunschweig, Germany.

Mohamed Rajik
Department of Microbiology, Faculty of Biotechnology and Biomolecular Sciences, University Putra Malaysia, UPM Serdang, Selangor, 43400, Malaysia.

Daniela Regenhardt
Environmental Microbiology Group, Helmholtz Center for Infection Research (HZI), Braunschweig, Germany.

Francesca Ricci
Dipartimento di Genetica e Biologia Molecolare, Sapienza Università di Roma, Roma, Italy.

Gianfranco Risuleo
Dipartimento di Genetica e Biologia Molecolare, Sapienza Università di Roma, Roma, Italy.

Eder L. Romero
Programa de Nanomedicinas, Universidad Nacional de Quilmes, Roque Saenz Peña 352, Bernal, Buenos Aires, Argentina.

Diana I. Roncaglia
Programa de Nanomedicinas, Universidad Nacional de Quilmes, Roque Saenz Peña 352, Bernal, Buenos Aires, Argentina.

Kennan Kellaris Salinero
Department of Plant and Microbial Biology, University of California, Berkeley, CA 94720, USA.
Yámana Science and Technology, Washington, DC 20009, USA.

C. A. Sargent
Department of Pathology, University of Cambridge, Cambridge CB2,1QP, UK.

Ajay Singh
The Department of Pathology, Case Western Reserve University, Cleveland, OH, USA.

Zacharias E. Suntres
The Novel Drug and Vaccine Delivery Systems Facility, Department of Chemistry and Biochemistry, Laurentian University, Sudbury, Ontario, Canada.
Medical Sciences Division, Northern Ontario School of Medicine, Lakehead University, Thunder Bay, Ontario, Canada.

Kenneth N. Timmis
Environmental Microbiology Group, Helmholtz Center for Infection Research (HZI), Braunschweig, Germany.

Stephan Trong
Genomics Division, DOE Joint Genome Institute, Walnut Creek, CA 94598, USA.

Marta Wanarska
Department of Microbiology, Chemical Faculty, Gdańsk University of Technology, Narutowicza 11/12, 80-952 Gdańsk, Poland.

Fei Wang
Drug Discovery and Design Centre, State Key Laboratory of Drug Research, Shanghai Institute of Material Medical, Graduate School of Chinese Academy of Sciences, Shanghai 201203, P.R. China.

Tiansong Wang
Department of Chemical Engineering, University of Washington, Seattle, WA, USA.
Department of Microbiology, University of Washington, Seattle, WA, USA.

Kaifeng Wu
Key Laboratory of Laboratory Medical Diagnostics, Ministry of Education, Faculty of Laboratory Medicine, Chongqing Medical University, Chongqing 400016, P.R. China

Qiangwei Xia
Department of Chemical Engineering, University of Washington, Seattle, WA, USA.
Department of Microbiology, University of Washington, Seattle, WA, USA.
University of Wisconsin-Madison, Department of Chemistry, Madison, WI, USA.

Hua Xie
Department of Oral Biology, University of Florida, Gainesville, FL, USA.

Nanlin Yin
Key Laboratory of Laboratory Medical Diagnostics, Ministry of Education, Faculty of Laboratory Medicine, Chongqing Medical University, Chongqing 400016, P.R. China.

Yibing Yin
Key Laboratory of Laboratory Medical Diagnostics, Ministry of Education, Faculty of Laboratory Medicine, Chongqing Medical University, Chongqing 400016, P.R. China.

J. F. Yuan
Key Lab of Agricultural Animal Genetics, Breeding and Reproduction of Ministry of Education, HuaZhong Agricultural University, 430070, P.R. China.
Department of Pathology, University of Cambridge, Cambridge CB2,1QP, UK.
College of Veterinary, South China Agricultural University, 510642, P.R. China.

Khatijah Yusoff
Department of Microbiology, Faculty of Biotechnology and Biomolecular Sciences, University Putra Malaysia, UPM Serdang, Selangor, 43400, Malaysia.
Institute of Bioscience, University Putra Malaysia, UPM Serdang, Selangor, 43400, Malaysia.

G. H. Zhang
College of Veterinary, South China Agricultural University, 510642, P.R. China.

S. J. Zhang
Key Lab of Agricultural Animal Genetics, Breeding and Reproduction of Ministry of Education, HuaZhong Agricultural University, 430070, P.R. China.
Department of Pathology, University of Cambridge, Cambridge CB2,1QP, UK.

Xuemei Zhang
Key Laboratory of Laboratory Medical Diagnostics, Ministry of Education, Faculty of Laboratory Medicine, Chongqing Medical University, Chongqing 400016, P.R. China.

Weiliang Zhu
Drug Discovery and Design Centre, State Key Laboratory of Drug Research, Shanghai Institute of Material Medical, Graduate School of Chinese Academy of Sciences, Shanghai 201203, P.R. China.

This page intentionally left blank

List of Abbreviations

AcCoA	Acetyl coenzyme A
AD	Activation domain
AIV	Avian influenza viruses
AKT1	v-Akt murine thymoma viral oncogene homolog 1
ALS	Amyotrophic lateral sclerosis
APLP1	Amyloid beta (A4) precursor-like protein 1
ARC	Archaeosomes
ATCC	American Type Culture Collection
BD	Binding domain
Bhp	Biphenyl/polychlorinated biphenyl
BHV-1	Bovine herpesvirus 1
BM	Black mud
Bp	Basepair(s)
BPG	Bisphosphatidyl glycerol
BSA	Bovine serum albumin
Bss	Benzylsuccinate synthase
BTEX	Benzene, toluene, ethylbenzene, and xylene compounds
BUB1	Budding uninhibited by benzimidazoles 1
CA	Cellular automaton
CALM3	Calmodulin 3
CAMH	Cation-adjusted Mueller-Hinton
CB	Constraint-based
CDC42	Cell division cycle 42
CDK4	Cyclin-dependent kinase 4
CDK7	Cyclin-dependent kinase 7
cDNA	Complementary deoxyribonucleic acid
CF	Cystic fibrosis
Chol	Cholesterol
CLSI	Clinical and Laboratory Standards Institute
CLSM	Confocal laser scanning microscopy
CLTB	Clathrin light chain
CLTC	Clathrin heavy chain
CNS	Central nervous system
COG	Clusters of orthologous gene
cRBCs	Chicken red blood cells

Ct	Threshold cycle
DAVID	Database for Annotation, Visualization and Integrated Discovery
DFO	Desferrioxamine
DMPC	1,2-Dimyristoyl-sn-glycero-3-phosphocholine
DNA	Deoxyribonucleic acid
DPPC	1,2-Dipalmitoyl-sn-glycero-3-phosphocholine
DSMZ	Deutsche Sammlung von Mikroorganismen and Zellkulturen
ED	Entner-Doudoroff
EE	Encapsulation efficiency
ESI-MS	Electrospray ionization-mass spectrometry
EST	Expressed sequence tag
FAC	Ferric ammonium citrate
FBA	Flux balance analysis
FBS	Fetal bovine serum
FBXW7	F-Box and WD repeat domain containing 7
FDR	False discovery rate
FGF	Fibroblast growth factor
FNR	False negative rate
FOS	v-Fos FBJ murine osteosarcoma viral oncogene homolog
F-PMB	Free polymyxin B
F-TOB	Free tobramycin
FVA	Flux variability analysis
GADD45	Growth arrest and DNA-damage-inducible alpha
GCs	Gray crystals
GPI	Glycosylphosphatidyl inositol
GPR	Gene-protein-reaction
GSS	Gerstmann-Straussler-Scheinker disease
HA	Hemagglutinin
HI	Hemagglutination inhibition
HK	Histidine kinase
HMM	Hidden Markov models
HPP	Hydroxyphenyl propionate
HPTS	8-Hydroxypyrene-1,3,6-trisulfonic acid
HS3ST5	Heparan sulfate (glucosamine) 3-O-sulfotransferase 5
HSPB2	Heat shock 27 kDa protein 2
HSPC	Hydrogenated phosphatidylcholine from soybean
HSPD1	Heat shock 60 kDa protein 1
HSV-1	Herpes simplex virus1
HTVS	High throughput virtual screening

HveC (PVRL1)	Herpesvirus entry mediator C (poliovirus receptor-related 1)
HveD (PVR)	Herpesvirus entry mediator D (poliovirus receptor)
ICL	Isocitrate lyase
ID2	Inhibitor of DNA binding 2
ID3	Inhibitor of DNA binding 3
ID4	Inhibitor of DNA binding 4
IPTG	Isopropyl-1-thio-β-D-galactopyranoside
IRPs	Iron regulatory proteins
KEGG	Kyoto Encyclopedia of Genes and Genomes
LANL	Los Alamos National Laboratory
LB	Luria–Bertani
LCP2	Lymphocyte cytosolic protein 2
LGA	Lamarchian genetic algorithm
LIP	Labile iron pool
LOWESS	Locally weighted scatterplot smoothing
LP	Linear programming
L-PMB	Liposomal polymyxin B
LPS	Lipopolysaccharide
LTA	Lipoteichoic acid
L-TOB	Liposomal tobramycin
MAPK	Mitogen-activated protein kinase
MBC	Minimal bactericidal concentration
mc	Metabolic cost
MCM7	Minichromosome maintenance complex component 7
MDR	Multi-drug resistant
MFC	Microbial fuel cells
MIC	Minimal inhibitory concentration
μL	Microliter(s)
MILP	Mixed-integer linear programming
MOSTI	Ministry of Science, Technology, and Innovation
mRNA	Messenger ribonucleic acid
MS	Mass spectrometry
MS^1	First stage of tandem mass spectrometry
MS^2	Second stage of tandem mass spectrometry
mTOR	Mechanistic target of rapamycin
NA	Neuraminidase
Na	Sodium
NAI	Neuraminidase inhibitors
NCBI	National Center for Biotechnology Information

NDV	Newcastle disease virus
NEFH	Neurofilament, heavy polypeptide
NEFL	Neurofilament, light polypeptide
NFE2L2	Nuclear factor (erythroid-derived 2)-like 2
NO	Nitrous oxide
OCV	Open circuit voltage
ONPGlu	*o*-Nitrophenyl-β-D-glucopyranoside
Orfs	Open reading frames
pAb	Polyclonal antibody
PBS	Phosphate buffered saline
PCNA	Proliferating cell nuclear antigen
PCR	Polymerase chain reaction
PDB	Protein Data Bank
PDCD8	Programmed cell death 8
PDH	Pyruvate dehydrogenase
PDMS	Polydimeyhylsiloxane
PEM	Proton exchange membrane
PG	Phosphatidylglycerol
PGD	Pseudomonas Genome Database
PGP-Me	Phosphatidylglycerophosphate-methyl ester
PHAs	Polyhydroxyalkanoates
PI	Post-inoculation
PIK3R1	Phosphoinositide-3-kinase regulatory subunit 1
PNPG	*p*-Nitrophenyl-β-D-galactopyranoside
PP	Pentose phosphate
PPP	Pentose phosphate pathway
PPP2CA	Protein phosphatase 2 catalytic subunit alpha isoform
PPP2CB	Protein phosphatase 2 catalytic subunit beta isoform
PPP3CA	Protein phosphatase 3 catalytic subunit alpha isoform
PRKACA	Protein kinase, cAMP-dependent, catalytic, alpha
PrP^{C}	Prion protein
PRRS	Porcine reproductive and respiratory syndrome
PRRSV	Porcine Reproductive, and Respiratory Syndrome Virus
PRV	Pseudorabies virus
PSSA	Pseudo steady-state assumption
PVRL3	Poliovirus receptor-related 3
Py	Polyomavirus
qRT	Quantitative real time

qRT-PCR	Quantitative real-time reverse transcriptase polymerase chain reaction
QS	Quorum sensing
QTL	Quantitative trait locus
rhDNase	Recombinant human DNase
RMSD	Root-mean-square deviation
ROS	Reactive oxygen species
RR	Response regulator
rRNA	Ribosomal ribonucleic acid
RSP	Rock-scissors-paper
RT-PCR	Reverse transcription-polymerase chain reaction
RV	Resveratrol
SBVS	Structure-based virtual screening
sCJD	Sporadic Cruetzfeldt–Jakob disease
SCX	Strong cation exchange
S-DGD	Sulfated diglycosyl diphytanylglycerol diether
SERPINE1	Plasminogen activator inhibitor, type I
SIH	Salicylaldehyde isonicotinoyhydrazone
SPP1	Secreted phosphoprotein 1
TCSs	Two-component systems
TEMED	N,N,N′,N′-Tetramethylethylenediamine
TGFβ	Transforming growth factor, beta
THBS4	Thrombospondin 4
TIGR-CMR	The Institute for Genomic Research Comprehensive Microbial Resource
TM	Transmembrane
Tmo	Toluene mono-oxygenase
TNFRSF	Tumor necrosis factor receptor superfamily
ToBiN	Toolbox for Biochemical Networks
TPL	Total polar lipids
tRNA	Transfer ribonucleic acid
VIMSS	Virtual Institute for Microbial Stress and Survival
VZV	Varicellovirus

This page intentionally left blank

Contents

Chapter 1

Microfabricated Microbial Fuel Cell Arrays

Huijie Hou, Lei Li, Younghak Cho, Paul de Figueiredo, and Arum Han

INTRODUCTION

Microbial fuel cells (MFCs) are remarkable "green energy" devices that exploit microbes to generate electricity from organic compounds. The MFC devices currently being used and studied do not generate sufficient power to support widespread and cost-effective applications. Hence, research has focused on strategies to enhance the power output of the MFC devices, including exploring more electrochemically active microbes to expand the few already known electricigen families. However, most of the MFC devices are not compatible with high throughput screening for finding microbes with higher electricity generation capabilities. Here, we describe the development of a microfabricated MFC array, a compact and user-friendly platform for the identification and characterization of electrochemically active microbes. The MFC array consists of 24 integrated anode and cathode chambers, which function as 24 independent miniature MFCs and support direct and parallel comparisons of microbial electrochemical activities. The electricity generation profiles of spatially distinct MFC chambers on the array loaded with *Shewanella oneidensis* MR-1 differed by less than 8%. A screen of environmental microbes using the array identified an isolate that was related to *Shewanella putrefaciens* IR-1 and *Shewanella* sp. MR-7, and displayed 2.3-fold higher power output than the *S. oneidensis* MR-1 reference strain. Therefore, the utility of the MFC array was demonstrated.

The MFCs are devices that generate electricity from organic compounds through microbial catabolism [1-3]. A typical MFC contains an anaerobic anode chamber and an aerobic cathode chamber separated by a proton exchange membrane (PEM), and an external circuit connects the anode and the cathode [4, 5]. Electrochemically active microbes ("electricigens") reside within the anaerobic anode chamber. Electrons, generated during microbial oxidization of organic compounds, are delivered to the MFC anode via microbial membrane-associated components [3, 6], soluble electron shuttles [7, 8], or nanowires [9, 10]. Biofilms that support close physical interactions between microbial membranes and anode surfaces are also important for MFC power output [11]. Electrons flow from the anode to the cathode through the external electrical circuit. In parallel, protons generated at the anode diffuse through the PEM and join the electrons released to the catholyte (e.g., oxygen, ferricyanide) at the cathode chamber [1]. This electron transfer event completes the circuit.

The MFCs have generated significant excitement in the bioenergy community because of their potential for powering diverse technologies, including wastewater treatment, and bioremediation devices [12, 13], autonomous sensors for long-term operations in low accessibility regions [14, 15], mobile robot/sensor platforms [16],

microscopic drug-delivery systems [17] and renewable energy systems [18]. In addition, MFCs hold significant promise for supporting civilian and combat operations in hostile environments [16]. Therefore, the development of efficient MFCs that are capable of producing high power densities remains an area of intense research interest. However, economical applications of existing MFCs are limited due to their low power output [19], which ranges from 100 to 1,000 W/m^3 [20, 21].

Important strategies for enhancing MFC performance include engineering optimized microbes (and microbial communities) for use in these devices [22] and improving cultivation practices for these organisms [23, 24]. To date, detailed description of individual microbe performance in MFCs has been limited to a surprisingly small number of organisms [25]. The MFCs that are fed by sediment and wastewater nutrient sources and that exploit mixed microbial consortia for electricity generation have been described [26, 27]. However, with the conventional two-bottle MFCs, characterization of the electrochemical activities of the microbial species in these consortia has not been possible because these conventional MFCs are not suitable for parallel analyses due to their bulkiness. To address this issue, MFC systems that support parallel, low cost, and reproducible analysis of the electrochemical activities of diverse microbes are required. High throughput microarrays, including DNA microarrays, protein microarrays, and cell arrays, are powerful platforms for screening and analyzing diverse biological phenomena [28]. Various MFC platforms, including miniature MFC devices that enable parallel comparison of electricity generation in MFCs, are emerging [29, 30]. However, state of the art microfabrication and highly integrated parallel measurement approaches [31, 32] have not yet been exploited to construct an MFC array with highly consistent architecture and performance.

Here we describe our development of a compact and user-friendly MFC array prototype capable of examining and comparing the electricity generation ability of environmental microbes in parallel. The parallel analyses platform can greatly speed up research on electricigens. Importantly, the array was fabricated using advanced microfabrication approaches that can accommodate scale-up to massively parallel systems. The MFC array consisted of 24 integrated cathode and anode pairs as well as 24 cathode and anode chambers, which functioned as 24 independent miniature MFCs. We validated the utility of our MFC array by screening environmental microbes for isolates with enhanced electrochemical activities. Our highly compact MFC array enabled parallel analyses of power generation of various microbes with 380 times less reagents, and was 24-fold more efficient than conventional MFC configurations. This effort identified a *Shewanella* isolate that generates more than twice as much power as the reference strain when tested in both conventional and microfabricated array formats.

MATERIALS AND METHODS

Twenty-four Well MFC Array Design

Figure 2A shows the schematic illustration of the MFC array. The array was microfabricated using micromachining and soft lithography techniques. The 24-well device was composed of layered functional compartments in which microbe culture

wells were embedded. Each microliter-scale microbe culture well was combined with individually addressable anode and cathode electrodes and functioned as a separate MFC. The layers included anode electrodes, anaerobic microbe culture chambers (anode wells), a PEM, cathode chambers, and cathode electrodes (Figure 2A). The assembled device (Figure 2B–E) with acrylic supporting frames was coupled to a load resistor circuit board and a digital multimeter through a computer controlled switch box module and a data acquisition system (Figure 2F).

Twenty-four Well MFC Array Electrode Layer Microfabrication

An acrylic master mold having 4 × 6 arrays of pillars (diameter: 7 mm, height: 4 mm) was fabricated with a rapid prototyping machine (MDX-40, Roland Inc., Los Angeles, CA). PDMS precursor solution (Sylgard 184, Dow Corning, Auburn, MI) prepared by mixing base and curing agent at 10:1 ratio (v/v) was poured onto the acrylic master mold. After curing for 30 min at 85°C, the resulting polymerized polydimeyhylsiloxane (PDMS) slab was peeled off, creating an inverse replica of the acrylic master mold. The cathode layer was prepared by aligning and permanently bonding a PDMS well layer onto a patterned electrode layer. Platinum loaded carbon cloth (10%, A1STD ECC, BASF Fuel Cell, Inc., Somerset, NJ) was cut to the size of a well (diameter: 7 mm) and bonded on top of the Au electrode pads in the cathode electrode layer using silver paste (Structure probe, Inc., West Chester, PA). Cathode and anode electrode layers of the 24-well MFC array were fabricated using standard microfabrication techniques. The fabricated cathode and anode electrode substrates had 24 individually addressable electrodes, each having an 8 mm diameter disk pattern. Wires were then soldered to all contact pads to provide electrical interconnects between the MFC arrays and the voltage measurement setup.

Assembly of the MFC Array System

The 24-well MFC array system consisted of a 24-cathode array layer, a cathode well layer, a PEM, an anode well layer, and a 24-anode array layer. Cathode layer consisted of a PDMS well layer permanently bonded on an electrode layer. Platinum (Pt) loaded carbon cloth was cut to the size of the well (diameter: 7 mm) and bonded on top of the Au electrode pads. The anode layer consisted of three layers: two PDMS layers fabricated as described above and an acrylic layer (8 mm thick) having 4 × 6 arrays of through-holes (7 mm diameter) fabricated by a rapid prototyping machine. The two PDMS layers were placed on both sides of the acrylic layer. The rigid acrylic layer served as a support layer that could be clamped tightly in the subsequent assembly step. The cathode layer, activated PEM, and the anode layer were then assembled together. To assemble these layers together, a top and bottom acrylic support frame that could be used to tightly clamp all layers together in between was cut out using a rapid prototyping machine. The sequence of images (Figure 2B–F) shows how all parts of a 24-well MFC array system was assembled.

Organisms, Media and, Growth Conditions

Shewanella oneidensis MR-1 was obtained from American Type Culture Collection (ATCC, Manassas, VA). Environmental bacteria used for screening were isolated from

eight different samples (soil and water) obtained from Lake Somerville (N30°30′09″ and E96°64′28″), Brazos River (N30°55′84″ and E96°42′24″; N30°62′64″ and E96°55′13″) and Lake Finheather (N30°64′93″ and E96°37′54″) around College Station, Texas.

Isolation and Pre-screening of Environmental Microbes

We performed a pre-screening for electrochemically active microbes. Each diluted sample was plated on nutrient agar and incubated under anaerobic conditions. The resulting 50–100 microbial colonies per plate were then used for plating on nutrient agar containing 100 μM Reaction Black 5, an azo dye that resulted in dark blue color of the media. After 3 days of incubation, a total of 26 colonies formed discoloration halos out of about 1,500 colonies plated for each of the eight environmental samples. The discoloration of the dye indicated reduction capability of the microbes. A total of 13 isolates were selected for MFC array screening. Un-inoculated medium was used as the negative control.

The 16s rDNA Amplification and Phylogenetic Analyses for Environmental Isolates

Colony PCRs were performed using different environmental isolates as the templates. The PCR products were then purified and sequenced with primers 11F and 1492R. The 16S rDNA sequences were BLAST searched against the GenBank database and the top hit for each isolate were used for alignment and phylogenetic tree generation. Sequences of the 16S rDNA of 15 members of genus *Shewanella* similar to 7Ca were aligned and phylogenetic tree was constructed among selected *Shewanella*. A matrix of pairwise genetic distances by the maximum-parsimony algorithm and the neighbor-joining method was used to generate phylogenetic trees.

The MFC Array Characterization and Data Acquisition

Two characterization methods were used to evaluate electricity generation from each of the 24 MFC wells. First, 24 1 MΩ fixed load resistors were connected to each of the MFC wells and voltage across these resistors were recorded. Load resistance of 1 MΩ was selected for MFC characterization because power output of *S. oneidensis* MR-1 at this resistance was close to maximum and the fabricated MFC array showed a steady state current output much faster than using resistors with lower resistances. A switch box module having an integrated digital multimeter (PXI-2575, PXI-4065, National Instruments, Austin, TX) and controlled through LabView™ (National Instruments, Austin, TX) was used to continuously measure voltages across the 24 load resistors that were connected individually to the 24 MFC array. The measured voltages were converted to current densities (mA/m^2, electrode area: 0.385 cm^2) using Ohm's law, and power densities were calculated using $P = VI/A$ (V: voltage, I: current, A: electrode area).

Full characterization of an MFC requires a current density versus power density plot, which can be obtained when measuring voltages across varying resistors. In this second characterization method, twenty-four 100 KΩ variable resistors (652-3296Y-1-104LF, Mouser Electronics, Mansfield, TX) were connected in series with twenty-four

2 MΩ variable resistors (652-3296Y-1-205LF, Mouser Electronics, Mansfield, TX) in pairs on a circuit board, connected correspondingly to the 24 MFC wells. For environmental screening of microbes using the MFC array, both the primary screening and the secondary confirmation started 1,000 min after loading microbes into the MFC array loaded with 1 MΩ resistors. One, 10, 20, 50, 100, 200, 500, 1,000, and 2,000 KΩ loading resistors were used and voltages across these resistors were continuously recorded.

RESULTS AND DISCUSSION

We recognized that selection of an appropriate anode material would be critical to the successful development of an MFC array and therefore initiated our studies by examining the performance of a commonly used anode material, carbon cloth in comparison to gold in a conventional MFC device (Figure 1). We used the model facultative anaerobe *S. oneidensis* MR-1 for these experiments because this organism had previously proven useful for the development of MFC applications [37]. The MFC power output was monitored for 5 hr after bacteria were introduced into the device. When the MFC was loaded with a 20 KΩ resistor, the gold electrode supported maximal power density of 3.77 ± 0.02 mW/m^2 at a current density of 16.47 ± 0.04 mA/m^2. A high standard deviation was observed (10% deviation). However, the MFC with gold anode displayed greater reproducibility (3.1% deviation). The open circuit voltage (OCV) of MFCs containing gold and carbon cloth anodes was 514 ± 12 mV (mean ± SE, n = 3) and 538 ± 51 mV (mean ± SE, n = 4), respectively. These results indicated that the OCV of the MFC with the gold anode was comparable to the corresponding OCV with the carbon cloth anode. However, OCV measurements with the carbon cloth anode displayed greater variance.

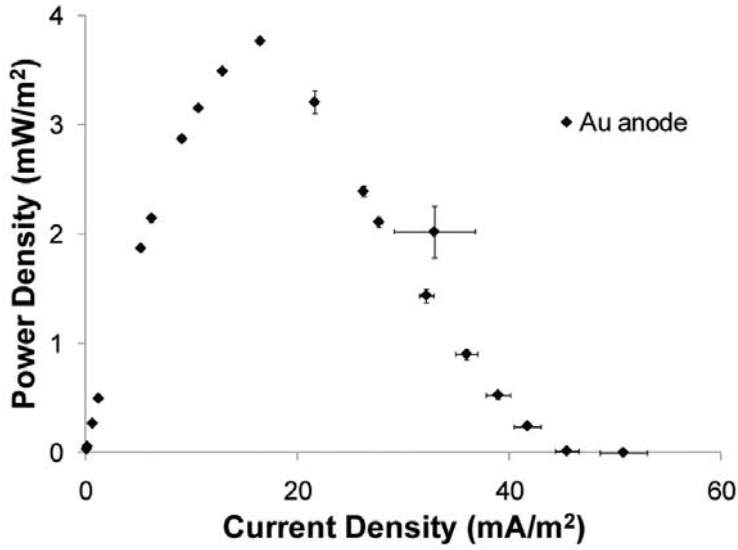

Figure 1. Au working as anode of MFC. Power density versus current density from an MFC with gold anode (n = 3).

An important hurdle to overcome in the development of MFC array systems is the identification of an electrode material that is durable, conductive, biocompatible, and easily fabricated [33]. Graphite, in the form of carbon cloth or graphite felt, has typically been the material of choice for the construction of MFC anodes, and conductive elements such as manganese, iron, quinines, and neutral red have been incorporated in graphite electrodes to significantly increase power output [33, 34]. However, graphite is not suitable for microfabricated MFC array systems [35]. The surfaces of graphite electrodes are non-uniform and difficult to pattern in small-scale devices. This non-uniformity thwarts efforts to compare performances between individual miniaturized MFCs. In addition, graphite materials are not compatible with most microfabrication technologies. Recently, gold has been identified as a potential material for MFC anode development [35]. Gold is highly conductive, can be vapor deposited, and is compatible with a wide array of conventional microfabrication modalities [36]. Thus, gold is a very attractive anode candidate for the development of an MFC screening platform. Our result showed that the MFC using gold as the anode material gave more reproducible results than its carbon cloth counterpart, a critical feature for side-by-side comparison in the MFC array. We therefore used gold as the anode material to develop the MFC array prototype.

Biofilms, when established on the anode of MFCs, enhance MFC performance when some microbial systems (including *S. oneidensis* MR-1) are employed. The enhanced performance has been suggested to result from the enhanced ability of biofilms to exploit close physical contacts between microbial membranes and the anode surface for electron transfer [11]. To investigate whether biofilms form on the surface of gold electrodes, light and fluorescence microscopy images of the electrode were captured 1 hr and 5 hr post-inoculation (PI). One hour PI, microbes started attaching to the gold electrode surface. Five hours later, an attached *S. oneidensis* biofilm was observed. Scanning electron micrographs of the electrode surface confirmed microbial attachment. Therefore, gold electrode supports *S. oneidensis* biofilm formation, and moreover, enables reproducible and consistent electrochemical activity to be measured when this model organism is used.

We were encouraged by our finding that gold electrodes can be employed in MFC devices, and exploited this material to develop an MFC array (Figure 2A). The array was successfully microfabricated using micromachining and soft lithography techniques. Performance and reproducibility of the MFC array were initially assessed by loading *S. oneidensis* MR-1 into the device and then measuring the electrical output. The current densities for negative control (un-inoculated medium) and *S. oneidensis* MR-1 chambers were 0.40 ± 0.01 mA/m^2 (mean ± SE, n = 4) and 1.80 ± 0.24 mA/m^2 (mean ± SE, n = 4), respectively (Figure 3A). Therefore the MFC array reproducibly measured the electrochemical activities of this microbial system (less than 14% of variance).

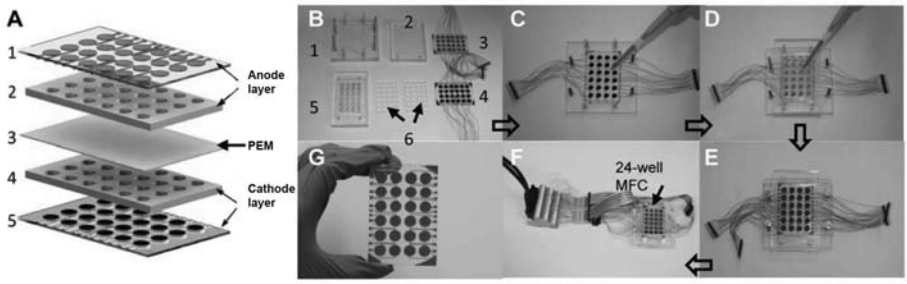

Figure 2. Illustration of the MFC array and its assembly steps. (A) Illustration of 24-well microbial fuel cell (MFC) array. Composed of an anode layer (1: anode electrode layer, 2: anode well layer), a proton exchange membrane (3: PEM), and a cathode layer (4: cathode well layer, 5: cathode electrode layer). (B)–(F) Microbial fuel cell array assembly. (B) Individual layers of the MFC array: acrylic support frames (1 and 2), cathode layer (3), anode electrode substrate (4), anode well layer (5 sandwiched by 6). (C) Assembly of the acrylic frame (1) with the cathode layer (3), followed by cathode solution loading. (D) Anode well layer and PEM assembly followed by microbe loading. (E) A fully assembled MFC array with the anode electrode layer (4) and acrylic frame (2) capping the anode wells. (F) Fully assembled MFC array connected to load resistors and a data acquisition system. (G) An MFC array device with no acrylic frame.

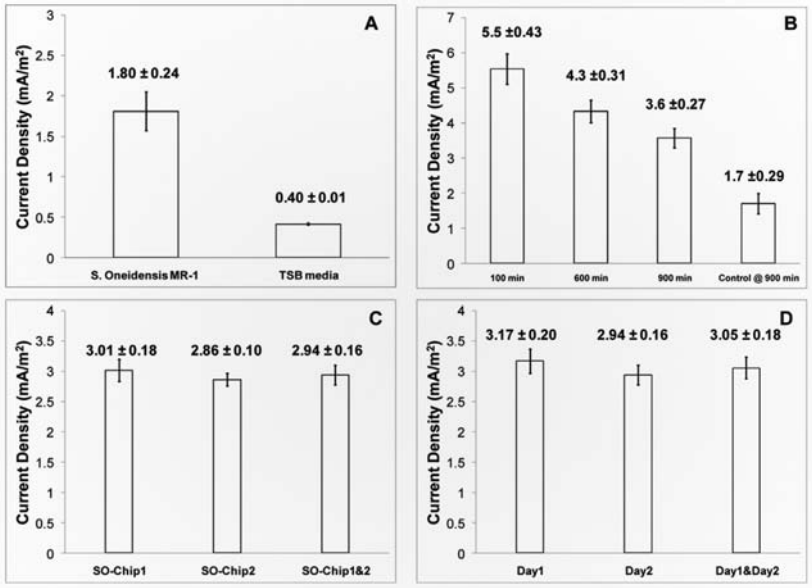

Figure 3. Characterization of current generated by *S. oneidensis* MR-1 in an MFC array. (A) Current densities generated by *S. oneidensis* MR-1 with PBS as the cathode solution at 350 min, TSB medium was used as the negative control (n = 4). (B) Repeatability of current densities generated by *S. oneidensis* MR-1 with ferricyanide as the cathode solution at different times after loading. TSB medium was used as the negative control (n = 5). (C) Chip-to-chip repeatability of current densities generated by *S. oneidensis* MR-1 with ferricyanide (100 mM) as the cathode solution at 1,000 min (n = 4 for each chip). (D) Batch-to-batch repeatability of current densities generated by *S. oneidensis* MR-1 with ferricyanide (100 mM) as the cathode solution at 1,000 min (n = 8 for each day). Means and standard errors were indicated above the bars (mean ± SE).

To increase the current, we used 100 mM ferricyanide at the cathode as the electrolyte due to the higher concentration of the electron acceptor in the cathode solution [4]. Under this condition, *S. oneidensis* MR-1 produced a current density of 5.54 ± 0.43 mA/m^2 (mean ± SE, n = 5) 100 min after loading microbes into the device (Figure 3B). Over time, the current density gradually dropped, but remained higher than that of the negative control wells containing medium only. The electricity generation profiles of spatially distinct wells measured at multiple time points during 15 hr of operation differed by less than 8%, demonstrating that individual wells of the MFC array displayed comparable performance characteristics.

Performances of the same microbial culture were also compared in different MFC arrays. Two arrays with the same configuration were tested with the same microbial culture (OD_{600} = 0.8) and showed current density of 2.94 ± 0.16 mA/m^2 (mean ± SE, n = 8) (Figure 3C). Thus the MFC arrays showed chip-to-chip variances of less than 5.4%. Performances of the same chip with microbial cultures of the same concentration (OD_{600} = 0.8) prepared on different days were also examined (Figure 3D). The current densities on two different days were 3.05 ± 0.18 mA/m^2 (mean ± SE, n = 16), showing a 5.9% variance. Therefore, the MFC array provided a platform for reproducible experimentation.

Encouraged by the performance and reproducibility of the MFC array, we examined whether the device could be employed to quickly screen environmental microbes for individual isolates that display enhanced electrochemical activities. A schematic representation of the screening process is shown in Figure 4A. We pre-screened ~12,000 microbes derived from environmental (water and soil) samples on solid medium containing Reaction Black 5, an azo dye that indicates electrochemically active organisms (Figure 4B,C) [39]. The 16S rDNA sequencing analysis of 26 hits obtained from the pre-screening plates revealed that the majority of the isolates (n = 10) were members of the Bacilli and γ-proteobacteria classes (Table 1). We then exploited the MFC arrays to characterize the electrochemical activities of several isolates. One isolate 7Ca reproducibly showed 266% higher power output than the *S. oneidensis* MR-1 reference strain in both the primary screening (Figure 4E) and the secondary confirmation with more replicates in the MFC arrays (Figure 4F). Phylogenetic analysis demonstrated that 7Ca was most closely related to *Shewanella putrefaciens* IR-1 (98% sequence similarity) and *Shewanella* sp. MR-7 (98% sequence similarity) (Figure 4D). The high power generation capability of 7Ca was further validated in 24-hr trials in a conventional H-type MFC system (Figure 4G) [6]. In our specific conventional MFC configuration, the maximum current density of 7Ca was 169.00 ± 10.60 mA/m^2, which was 217% higher than the current density (78.00 ± 7.30 mA/m^2) generated by the *S. oneidensis* MR-1 control. The maximum power density of 7Ca was also 233% higher than this reference strain. Although we used gold as the anode material in the MFC array and carbon cloth as the anode material in the H-type MFC system, the power density increases of 266% in the MFC array and 233% increase in the H-type MFC system showed that findings in our MFC array system can be translated to larger scale conventional systems. Thus, insights garnered using gold anodes in miniaturized MFCs can be transferred to conventional MFC formats using carbon anodes.